# A NOVEL TECHNIQUE FOR IDENTIFYING THE INDIVIDUAL REGIONS OF THE HUMAN COLON AT CT COLONOGRAPHY

**R J T Sadleir[1], P F Whelan[1], J F Bruzzi[2], A C Moss[2], H M Fenlon[2], P MacMathuna[2]**

[1]**Dublin City University, Ireland**
[2]**Mater Misercordiae Hospital, Ireland**

## INTRODUCTION

Colorectal cancer is a major cause of cancer related death worldwide. This type of cancer can be avoided if precursor polyps are detected and removed early in their course. Regular screening is required to facilitate the early detection of colorectal polyps. At present the most sensitive screening technique is *conventional colonoscopy* (CC). This is a highly invasive procedure involving an endoscopic examination of the colon. CC is not highly regarded among potential screening candidates due to the invasive nature of the examination and in rare cases complications may arise, the most significant being bowel perforation which can result in mortality.

*Computed tomography colonography* (CTC), also known as *virtual colonoscopy* (VC), is a new, non-invasive colon imaging technique that was first described by Vining et al (1) in 1994. A CTC examination is performed by indirectly inspecting the colon using images acquired from an abdominal *computed tomography* (CT) scan of a suitably prepared patient. Scans are generally performed using both prone and supine positioning in order to reduce the effects of residual material in the colon. Results from a major study carried out between March '97 and January '99 by Fenlon et al (2) show that CTC and CC have similar efficiencies for the detection of significant polyps, i.e. those where the probability of cancer is high.

CTC has several major benefits over CC. Firstly, It is noninvasive, this has major implications in relation to patient acceptance. In addition CTC has higher completion rates compared to conventional colonoscopy and can visualise the entire colon (from rectum to caecum) even in the presence of large obstructions that cannot be traversed endoscopically (3). It should also be noted that a CTC examination is not limited to the colon, in fact, the entire abdomen can be examined. This can lead to significant extracolonic findings that would have been missed at CC (4). Finally and most importantly, custom image and volumetric data analysis software and be readily employed to enhance the CTC process.

The most significant enhancements to date include alternative visualisation techniques (e.g. flattening of the colon (5)), digital cleansing (6) thus removing the need for cathartic preparation and most recently *computer aided diagnosis* (CAD) of colorectal polyps (7, 8). As CTC evolves as an accepted colon imaging technique further enhancements will be introduced. This paper describes one such enhancement; a technique for automatically identifying each of the individual colonic regions. This novel technique, which will be referred to as sub-segmentation, has been developed to complement automatic diagnosis by providing meaningful information about the location of automatically detected colorectal neoplasia.

## OVERVIEW

The human colon is divided into five anatomical regions, these are the: caecum & ascending colon, transverse colon, descending colon, sigmoid colon and rectum. From the ideal model of the colon (see Figure 1(a)) it is apparent that each of these regions represents either a horizontally or vertically aligned colonic segment. Furthermore, the junction between each of these regions is charactorised by a significant change in direction, or flexure. There are four flexures in total, these are the: hepatic ($P_{hep}$), splenic ($P_{spl}$) and sigmoid ($P_{sig}$) flexures and the rectosigmoid junction ($P_{rec}$) which will also be classified as a flexure for the purpose of this discussion.

In reality the shape of the human colon can deviate significantly from the ideal model (see Figure 1(b)). Kinks and loops are introduced over time and the colon invariably becomes distorted with age. The general shape of the colon is retained to some extent and can still be identified, however the task of automatic flexure detection is compounded by the frequency and magnitude of the colonic distortions. The remainder of this paper describes a series of techniques that can be used to reliably and accurately detect the four flexure points from real patient data even in the presence of significant colonic distortions. Accurate identification of these flexures is required to facilitate colon lumen sub-segmentation.

## PREPROCESSING

A CTC dataset is obtained by performing an abdominal CT scan of a suitably prepared patient. The region that must be scanned is determined by examining a scout X-ray of the patient's abdomen, this

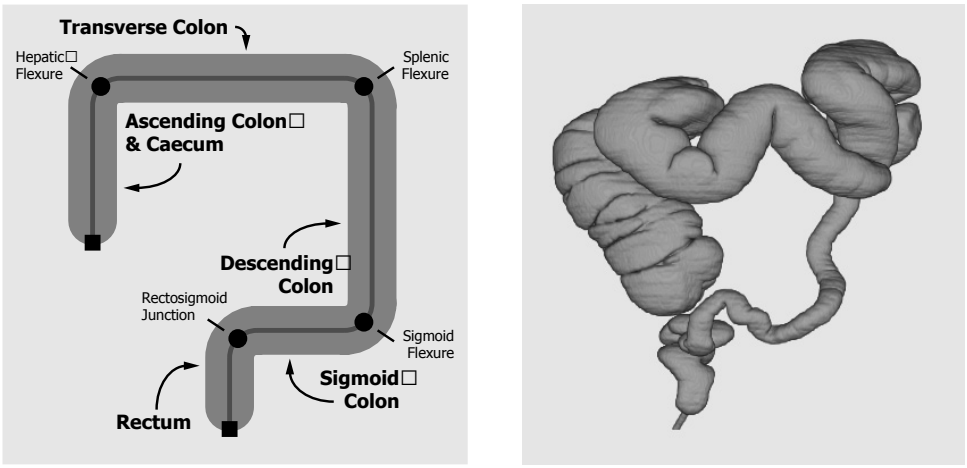


(a) (b)

Figure 1: Anatomy of the colon: (a) An illustration of the ideal colon where all colonic segments and flexures have been identified (b) An example of an actual human colon which has been segmented from a CTC dataset.

insures that the entire colon is imaged at CT. In general, a CTC dataset consists of approximately 300 DICOM compliant axial images, each image contains 512×512 pixels and pixel intensities can range from approximately -1500HU (air) to +1000HU (bone). Most of the information contained in a CTC dataset is not required for sub-segmentation, in fact, the flexure points can be identified by examining a relatively compact representation of the colon lumen that retains most of the original shape information. The centreline of the colon represents the shortest path between the two most distal points of the colon that is located at the furthest distance from the colon wall and so, meets these criteria. This section describes how the centreline of the colon is calculated from a CTC dataset.

### Segmentation

The voxels that represent the colon lumen must be identified prior to the calculation of the centreline. This is achieved using segmentation. The segmentation process involves the extraction of a binary model of the colon lumen from the original CTC dataset. Seeded region growing can be used to perform this task (9). The initial seed point(s) can be either user defined or automatically detected. The technique described here utilises an automatically detected seed point located in the rectum, this is the first endpoint of the colon ($EP_{rec}$). The region growing process is initiated from this point and continues until all contiguous voxels below a predetermined threshold (-800HU) are identified. In addition to segmenting the colon lumen, the region growing process is also used to identify a point in the caecum ($EP_{cae}$) that is furthest from $EP_{rec}$, this is the second endpoint of the colon.

### Centreline Calculation

The centreline is subsequently calculated from the segmented colon lumen using a modified version of 3D topological thinning (10). Standard 3D topological thinning (11) involves the removal of successive layers of surface voxels from the binary object being thinned. This process continues until certain topological and geometric constraints are violated. Extraneous loops may be present in the resulting centreline due to holes in the original binary object. In the case of the colon lumen these holes may be due to the Haustral folds. The final centreline, obtained by removing all extraneous loops, represents the path between the two most distal points of the colon that is furthest from the colon wall. Standard 3D topological thinning is an extremely slow process, so, in order to increase performance several optimisation techniques are employed. These include surface voxel tracking (12) and partial precalculation of results. The final centreline calculated using the optimised thining algorithm provides an accurate description of the colon using a relatively small number of data points.

## FLEXURE DETECTION

The centreline consists of a set of 3D points. These points can be readily analysed to determine changes in direction, thus facilitating automated flexure detection. As mentioned earlier, real human colons deviate significantly from the ideal model and as a re-

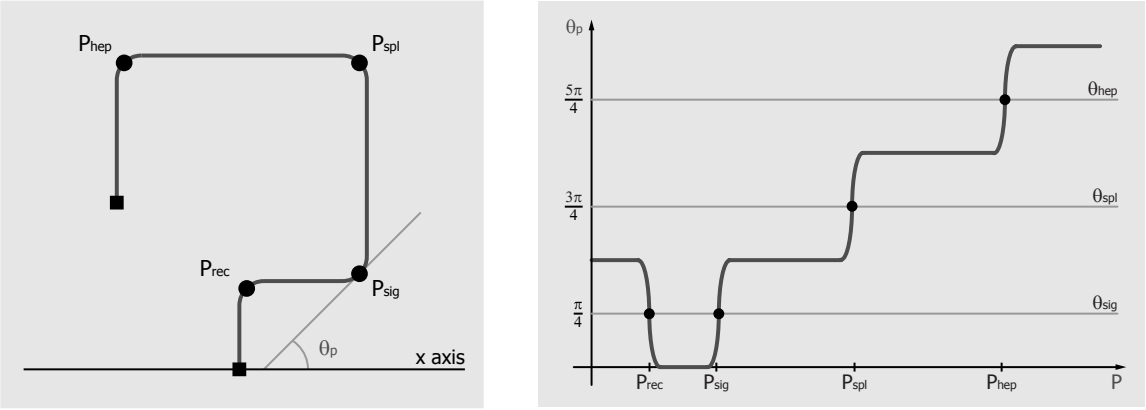


(a) (b)

Figure 2: Flexure detection theory: (a) The centreline of the ideal colon (see Fig. 1(a)) and (b) a graph of adjusted values of $\theta_p$ for each point $p$ in the centreline

sult steps must be taken to simplify the centreline in order to assist automatic flexure detection.

The colon is generally observed from a coronal perspective and although deviations may be present in the sagittal plane these do not have a significant influence on the location of the colonic flexures. Sagittal deviations in the centreline points can be ignored by simply projecting the centreline points from XYZ space (3D) onto the XZ plane (2D). Reducing the dimensionality of the centreline points in this manner decreases the amount of information required to describe the centreline while retaining much of the important shape information.

The projected centreline still retains the distortions described earlier. These distortions must be eliminated, or at least their magnitude must be reduced, so that the flexure points can be reliably detected. If the colon centreline is treated as signal then the kinks and loops represent noise. It is apparent that the frequency of this noise is significantly higher than the frequency of the underlying signal, i.e. the undistorted colon centreline. High frequency noise of this type can be suppressed by passing the data points through a symmetrical lowpass filter. In the case of the colon centreline, lowpass filtering is achieved by calculating the average location of each centreline point over a certain range $W$ (the filter width) i.e. $(x_p, z_p) \rightarrow (\bar{x}_p, \bar{z}_p)$. The filtering process is illustrated in Fig. 3, it is obvious that the filtered centreline (b) conforms much better to the ideal model that the original centreline (a).

The four flexures can be reliably identified by examining the retrograde (rectum to caecum) direction of the filtered 2D representation of centreline at each point. An approximation of the centreline direction can be obtained by calculating discrete first derivative ($\frac{dz}{dx}$), i.e the slope of the tangent to the centreline. The tasks of filtering and differentiating can be combined by calculating the change in the $x$ position ($\triangle x_p$) and the change in $z$ position ($\triangle z_p$) over a number of points, the number of points must be the same as the lowpass filter width $W$.

$$\triangle x_p = \sum_{i=p-\frac{W-1}{2}+1}^{p+\frac{W-1}{2}} x_i - x_{i-1} \tag{1}$$

$$\triangle z_p = \sum_{i=p-\frac{W-1}{2}+1}^{p+\frac{W-1}{2}} z_i - z_{i-1} \tag{2}$$

An approximation of the angle between the tangent to the centreline and the the $x$ $axis$ ($\theta_p$) can then be calculated for each of the centreline points.

$$\theta_p = \tan^{-1}\left(\frac{\triangle z_p}{\triangle x_p}\right) \tag{3}$$

The resulting value for $\theta_p$ will be in the range $-\frac{\pi}{2} \rightarrow \frac{\pi}{2}$. It is possible to adjust this value to the range $0 \rightarrow 2\pi$ by examining the discrete second derivative of the centreline ($\frac{d^2z}{dx^2}$). The values of $\theta_p$ for the ideal colon centreline are plotted in Fig. 2(b).

It is apparent from an examination of the ideal centreline (see Fig. 2(a)) that the flexure points are located where the centreline transitions from horizontally to vertically aligned colonic segments and vice

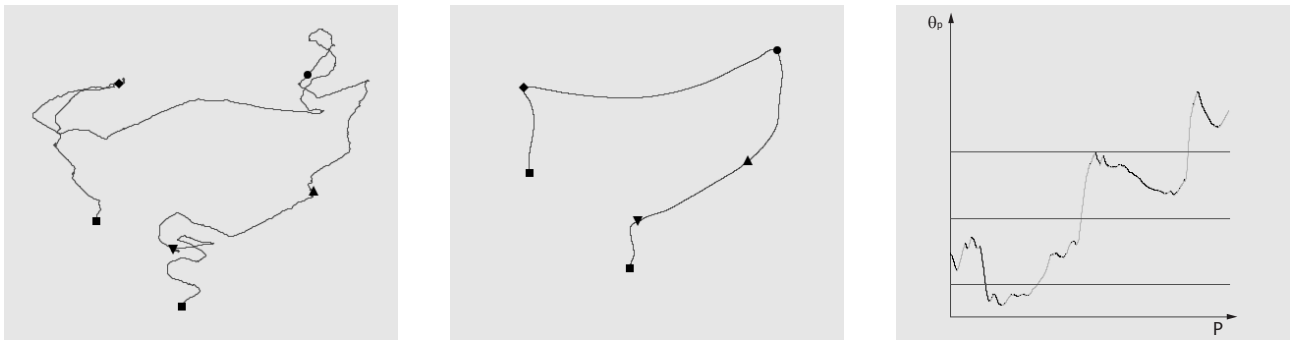


(a) (b) (c)

Figure 3: Flexure detection process: (a) The original colon centreline (b) A filtered version of the original centreline ($W = 319$) (c) A plot of $\theta_p$ against $p$ for the filtered centreline. [Flexure key: $\nabla = P_{rec}$, $\triangle = P_{sig}$, $\bigcirc = P_{spl}$ & $\diamondsuit = P_{hep}$]

versa. Consider the splenic flexure, this is located where the direction of the centreline changes from $\frac{\pi}{2}$ (ascending colon) to $\pi$ (transverse colon). The ideal splenic flexure is located midway between these two angles, at the point where the $\theta_p$ curve intersects with the line at $\frac{3\pi}{4}$, i.e. the splenic angle ($\theta_{spl}$). Similarly the hepatic angle ($\theta_{hep}$) is at $\frac{5\pi}{4}$ and the sigmoid angle ($\theta_{sig}$), which identifies both the rectosigmoid junction and the sigmoid flexure, is at $\frac{\pi}{4}$. It is possible to differentiate between the sigmoid flexure and the rectosigmoid junction by examining the discrete second derivative of the centreline at each of these points. In the case of the rectosigmoid junction, the value of $\theta_p$ transitions from $\frac{\pi}{2} \rightarrow 0$, therefore the value of $\theta_p$ is decreasing and the discrete second derivative of the centreline will be negative at this point. Note that the opposite is true for the sigmoid flexure.

In the final system the width of the lowpass filter $W$ is initialised at a low value and then increased until all flexure points are identified. The location of each flexure point is recorded immediately after it has been uniquely detected, this insures that regions with a large number of strong deviations do not affect those which are relatively smooth, thus insuring maximum sensitivity for individual flexure point detection. The flexure detection process terminates when the last flexure point has been uniquely identified. The automatically detected flexure points are ultimately used to facilitate the sub-segmentation of the colon lumen.

## RESULTS

The sub-segmentation technique described in the previous section was evaluated using five CTC datasets which were obtained from the Department of Radiology at the Mater Misercordiae Hospital in Dublin. These datasets were obtained by scanning a cohort of patients of mixed sex all of whom were above 50 years of age. The age of the cohort insured that a significant number of deviations would be present in the test set of colons.

The sub-segmentation software was implemented using Java (J2SEv1.3) and tested on a standard 700Mhz, 512MB PC workstation. The four flexures were uniquely detected from each of the relevant colon centrelines in an average time of 2.55 seconds (range 0.55 - 4.04). No false positive detections were made. The position of the automatically detected and manually selected flexure points $d_p$ was calculated relative to $EP_{rec}$.

$$d_p = \sum_{i=1}^{p} \sqrt{\begin{array}{l}(v_x(x_i - x_{i-1}))^2 + \\ (v_y(y_i - y_{i-1}))^2 + \\ (v_z(z_i - z_{i-1}))^2\end{array}} \qquad (4)$$

The symbols: $v_x$, $v_y$ and $v_z$ represent the voxel dimensions. For all datasets used in this study these values were approximately 0.74mm, 0.74mm and 1.5mm respectively. The mean error (ME) was then calculated for each of the automatically detected flexure points, this was found to be 31.03mm. The most accurately detected point was the hepatic flexure (ME = 7.53mm) whereas the least accurately detected point was the sigmoid flexure (ME = 54.30mm). It should be noted that it is impossible to unique identify the flexure points and that mean errors of this magnitude are acceptable. In addition, these errors should be considered in relation to the average colon length (including rectum) which was approximately 2000mm.

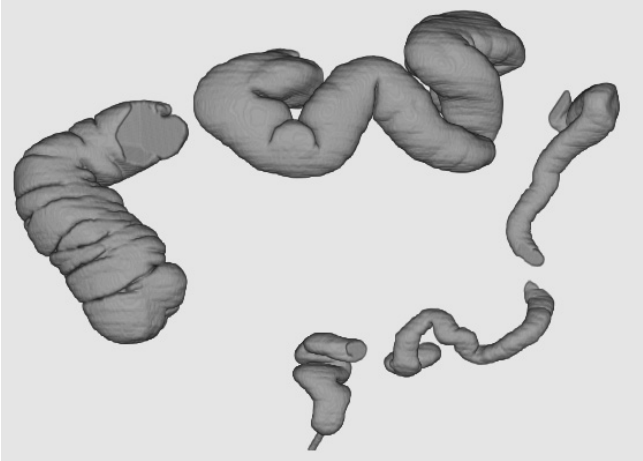

Figure 4: A sub-segmented version of the colon lumen illustrated in Fig. 1(b)

## CONCLUSION

A straightforward technique for sub-segmentation of the human colon has been described. Using this technique it is possible to automatically identify each of the individual colonic regions. Sub-segmentation can be used in conjunction with CAD, thus facilitating automated reporting at CTC. The sub-segmentation technique described in this paper has been evaluated using real patient data. In each case the colon lumen was accurately sub-segmented even in the presence of significant colonic distortions. The research described in this paper is an extension of our work in the area of colon centreline calculation (10). Sub-segmentation is a good example of how the colon centreline can be analysed in order to obtain additional information about the structure of the colon, thus enhancing the CTC process.

## ACKNOWLEDGMENTS

This work was supported by grants from the Irish Cancer Society and the Health Research Board.

## REFERENCES

1. Vining, D.J., Gelfand, D.W., Bechtold, R.E., Scharling, E.S., Grishaw, E.K., Shifrin, R.Y., 1994, AJR, 162, Supplement, 104 (abstract)

2. Fenlon, H.M., Nunes, D.P., Schroy, P.C., Barish, M.A., Clarke, P.D., Ferrucci, J.T., 1999, New Engl J Med, 341, 1496-1503

3. Fenlon, H.M., McAneny, D.B., Nunes, D.P., Clarke, P.D., Ferrucci, J.T., 1999, Radiology, 210, 423-428

4. Hara, A.K., Johnson, C.D., MacCarty, R.L., Welch, T.J., 2000, Radiology, 215, 353-357

5. Haker, S., Angenent, S., Tannenbaum, A., Kikinis, R., 2000, IEEE T Med Imaging, 19, 665-670

6. Zalis, M.E., Hahn, P.F., 2001, AJR, 176, 646-648

7. Gökturk, S.B., Tomasi, C., Acar, B., Beaulieu, C.F., Paik, D.S., Jeffrey, R.B., Yee, J., Napel, S., 2001, IEEE T Med Imaging 20, 1251–1260

8. Yoshida, H., Nappi, J., 2001, IEEE T Med Imaging 20, 1261-1274

9. Sato, M., Lakare, S., Wan M., Kaufman, A., Wax M., 2001, IEICE T Inf Syst, E84D, 201–208

10. Sadleir, R.J.T., Whelan, P., 2002, "Colon centreline calculation for CT colonography using optimised 3D topological thinning", *in Proc* 1st International Symposium on 3D Data Processing Visualization and Transmission, 800-803

11. Tsao, Y.F., Fu, K.S., 1981, Comp Graph Im Proc, 17, 315-331

12. Ge, Y., Stelts, D.R., Wang, J., Vining, D.J., 1999, J Comput Assist Tomo, 23, 786-794